ADVANCED MATERIALS
www.advmat.de

Carbon-Carbon Contacts for Robust Nanoelectromechanical Switches

*Owen Loh, Xiaoding Wei, John Sullivan, Leonidas E. Ocola, Ralu Divan, and Horacio D. Espinosa**

Nanoscale electromechanical (NEM) contact switches are attractive complements or alternatives to solid-state silicon electronics for their minimal electrical leakage, sharp switching, and temperature and radiation tolerance. Despite the potential advantages, only limited reports exist of these devices operating reliably beyond a few cycles. This is especially true for highly-scaled devices made from carbon nanotubes (CNTs) or nanowires. Here we report a novel material selection, namely the use of carbon-carbon contacts, to improve the reliability of these devices. NEM contact switches are constructed using a CNT as an active element which makes contact with a conductive diamond-like carbon (DLC) electrode when the switch is closed. Switch response times are characterized and basic logic operations demonstrated from pairs of switches. We find that the robust carbon-carbon contact, which is facile to apply to a variety of reported nanoelectromechanical architectures currently using metal electrodes, endures prolonged cycling without failure. This in turn represents a viable means to improve the reliability of these diverse, widely-pursued nanoscale devices ranging from single-nanostructure switches to massively parallel arrays through improved material selection.

Solid-state electronics are well established thanks in part to scalable manufacturing processes and reliable performance. However, as these devices continue to scale and their applications become increasingly demanding (e.g., increasing performance while greatly reducing power consumption), new technologies are sought to sustain their advance. NEM contact switches have a physical gap separating their terminals (see for example **Figure 1**a), which greatly reduces leakage current[1–4] and enables ultra-low power consumption with sub-threshold slopes well below the theoretical limit of 60 mV/decade for conventional CMOS.[3,5] Thus when combined with conventional CMOS in hybrid systems, for example by using NEM switches in the pull-down network of CMOS logic gates[3] or memory cells,[6] they can dramatically reduce the power consumption of these hybrid systems (predicted reduction in static power dissipation of nearly 100% and switching power reduced by 80%) while enabling continued scaling of the silicon.[3,7,8] Additionally, NEM switches have proven relatively insensitive to radiation,[9] temperature,[2] and external electric fields,[10] conditions which pose further challenges to conventional solid-state devices in aerospace, defense, and other environmentally demanding applications. As such, NEM switch architectures are widely pursued to advance both hybrid and standalone transistor, memory, logic, and sensing applications.[1,3,4,9,11–23]

Despite their potential advantages, NEM switch technologies have yet to widely mature. This is largely the result of challenges in manufacturing and reliability.[24] Difficulties associated with manipulating individual nanostructures into well-ordered arrays greatly limit scalable production of these devices. This is compounded by a need for ultra-small devices (with typical critical dimensions on the order of 1 to 10 nm) to achieve actuation voltages in the 1 V range.[25,26] Additionally, a number of prevalent failure modes intrinsic to the materials commonly used greatly affect reliability, including damage from electrical discharge, and irreversible stiction preventing reopening of the switch.[18,25] Jang et al. used electrodes with ultrathin oxide coatings to limit electrical discharge.[5] This enabled repeatable operation of nanoscale thin film beam structures for several hundred cycles before the switching characteristics began to deteriorate as the thin coating wore away.[5,11] Likewise, switches cut from dense films of CNTs operated successfully through tens of cycles before sticking irreversibly.[27] Ward et al. used voltage pulses to break the stiction in devices constructed from suspended ribbons of dense CNTs, enabling millions of cycles without failure.[13]

The aforementioned failure modes become increasingly prominent as the active elements in these electromechanical devices scale downward from micromachined beams and multi-nanostructure ensembles to individual carbon nanotubes[4,10,18,21,28–31] or nanowires.[15,16] To the best of our knowledge, there are no reports of such devices operating repeatedly through extended cycling. For example, relays composed of individual cantilevered or suspended CNTs tended to stick irreversibly or suffer from ablation of the CNT due to electrical discharge upon closing,[18,21,28,29] resulting in rapid degradation of switching characteristics with repeated actuation. Monolayer electrode coatings helped to reduce stiction, but also degraded with repeated switching.[32] Switches made from vertically-aligned CNTs suffered from similar burnout and

O. Loh, X. Wei, Prof. H. D. Espinosa
Dept. of Mechanical Engineering
Northwestern University
2145 Sheridan Rd., Evanston, IL 60208-3111, USA
E-mail: Espinosa@northwestern.edu
J. Sullivan
Center for Integrated Nanotechnologies
MS 1304, PO Box 5800
Sandia National Laboratories
Albuquerque, NM 87185-1304, USA
L. E. Ocola, R. Divan
Center for Nanoscale Materials
Argonne National Laboratories
9700 S. Cass Ave., Building 440, Argonne, IL 60439-4806, USA

DOI: 10.1002/adma.201104889

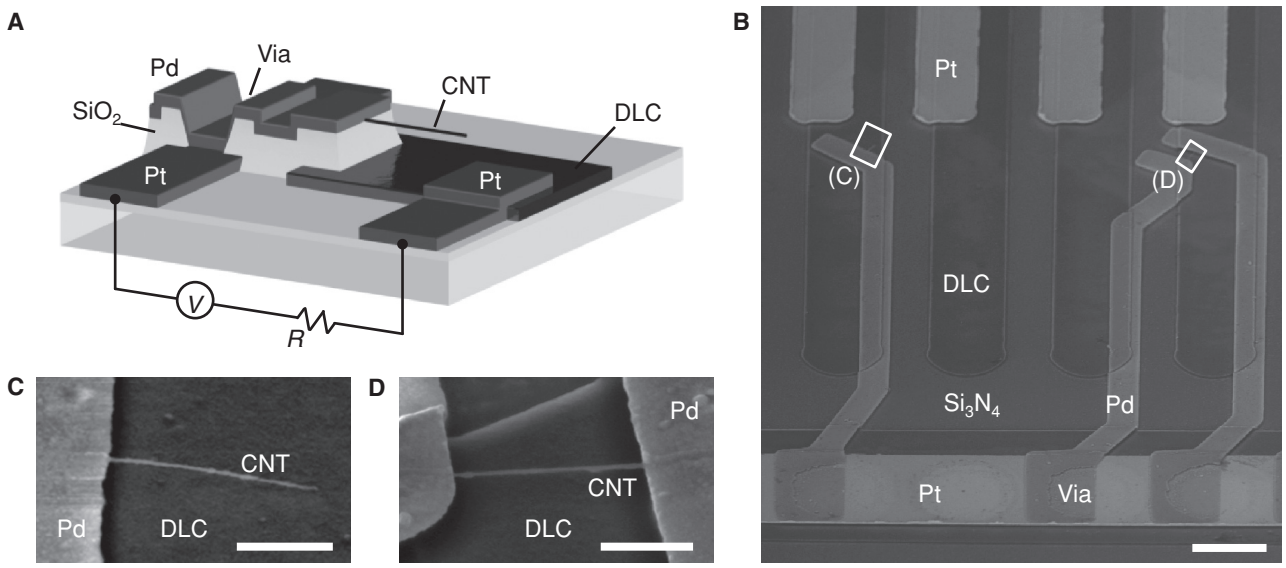

Figure 1. Carbon-carbon nanoelectromechanical switches consisting of an individual carbon nanotube and a diamond-like carbon contact electrode. (A) Schematic of the NEM switch architecture. The CNT is cantilevered or suspended over a DLC electrode. When an electrical bias is applied, electrostatic forces deflect the CNT into contact with the DLC electrode. (B–D) Representative scanning electron micrographs showing a cantilevered switch in the closed/on position (C) and a suspended switch in the open/off position (D). Scale bars are 5 µm, 1 µm, and 500 nm respectively. Substrate is tilted 52° about the horizontal axis of each image.

stiction in some cases,[4] though the use of a third actuation terminal helped to reduce the occurrence. Telescopic switches constructed from multi-walled CNTs enabled ultra-small device pitches on the order of 200 nm, but burning of CNT shells with repeated actuation was also reported.[30] Together, these failure modes pose a prominent roadblock to realizing reliable integrated NEM-CMOS hybrids.

In this paper, we demonstrate how a facile change in material selection for the physical contact in NEM switches can significantly improve the reliability of NEM switches for use in hybrid NEM-CMOS devices or select standalone applications. The relatively high contact resistance and low adhesive forces between the CNT and DLC electrode were previously shown to greatly reduce the occurrence of short-term failure of CNT-based NEM switches due to electrical discharge or irreversible stiction in comparison to similar device architectures employing more common metal electrodes.[18] However, we find here that the mechanical robustness of the DLC electrodes themselves, when combined with the use of high-quality CNTs with minimal defects, in fact enables millions of highly consistent switching cycles. Furthermore, because this change requires only a modification in the electrode material, it is directly applicable to other reported devices ranging from ultra-small devices constructed with individual CNTs or graphene, up to devices using hundreds of CNTs in parallel (e.g., to achieve higher current flows). Finally, the use of DLC is expected to be more conducive to CMOS-compatible fabrication means in comparison to more commonly used gold thin film NEM switch electrodes which could significantly limit the thermal budget or cause diffusion or contamination concerns.

As a platform for this study, carbon-carbon NEM switches (Figure 1A-B) consisting of an individual multi-walled CNT as an active element which was either cantilevered (Figure 1C) or suspended (Figure 1D) over a conductive DLC electrode (~50 Ω-cm resistivity, controlled via nitrogen doping[33]) were fabricated (see Figure S1 in Supporting Material). Characteristic Raman spectra obtained from the DLC electrodes (Supporting Figure S2) suggest an sp^3-hybridized carbon content of approximately 80% (i.e., largely amorphous diamond[34]). The switches were actuated by applying an electrical bias between the CNT and the opposing DLC electrode, resulting in a carbon-carbon contact when the switch was closed (see Figure 1C).

Cantilevered carbon-carbon NEM switches were characterized first. **Figure 2**A,B shows a cantilevered device and the corresponding current-voltage response. A characteristic hysteretic loop is observed, which is similar to those observed in other NEM switches.[5,11,16,18,27,29,31] A sharp off-on transition occurs at a pull-in voltage of V_{PI} = 23.4 V, followed by a similarly well-defined on-off transition as the voltage is subsequently ramped down below the pull-out voltage (V_{PO}). In general, experimentally-observed pull-in voltages matched well with those predicted theoretically for devices of this geometry.[35,36]

The response time of the cantilevered devices was estimated following the method of Kaul et al.[37] A step input was applied to the device using a function generator and the corresponding output monitored through a buffer circuit and oscilloscope (see Supporting Information and Figure S7 for full description). We then define the response time as the delay between the point at which the input signal reaches pull-in level (23.4 V, the point at which pull-in is assumed to initiate, see Figure 2B) and the time at which there is measurable output from the device. Figure 2C shows the input and output signal in response to the step input. There is a well-defined delay of 10 ± 2 ns between the time the reference input signal first reaches pull-in level and the point at which the output begins to rise. Here the error considers potential uncertainty in the point at which pull-in

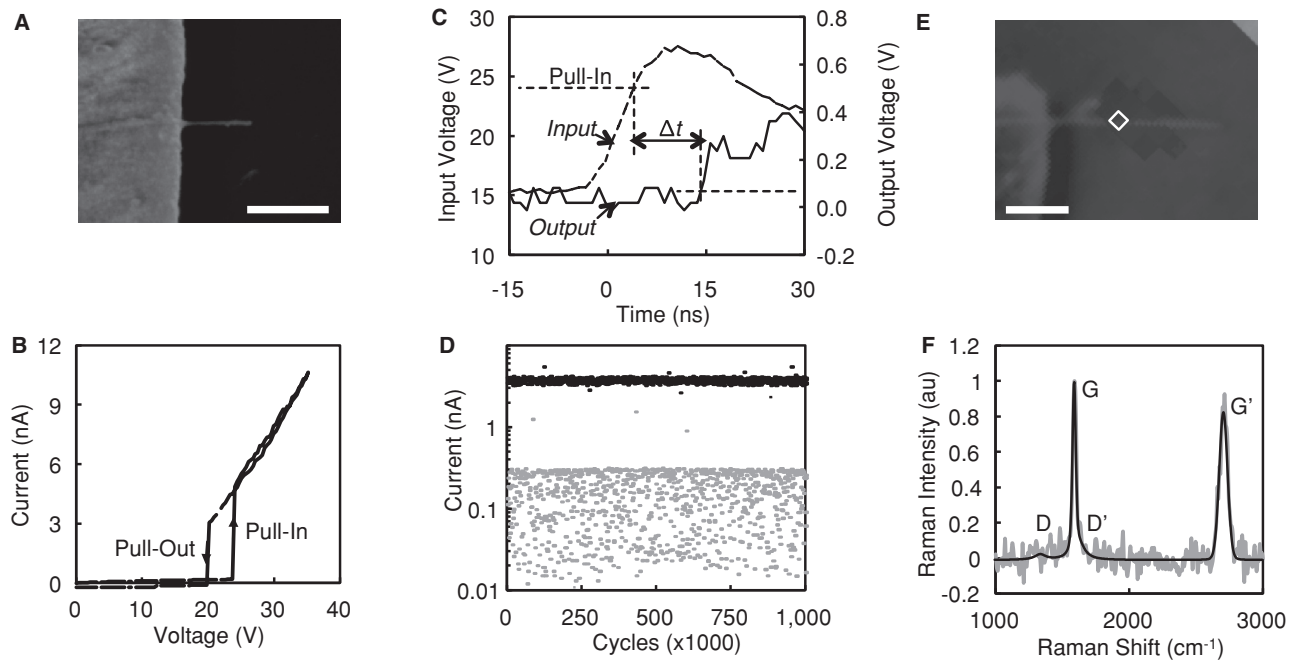

Figure 2. Characterization of cantilevered carbon-carbon NEM switches. (A) Scanning electron micrograph of a cantilevered device. The CNT is fixed at one end by a palladium contact and cantilevered over a DLC electrode. Scale bar is 500 nm. Substrate is tilted 52° about the horizontal axis of the image. (B) Current-voltage response of the device shown in (A). (C) Plot of step input signal and switch output from the device shown in (A) used to characterize switch response time. There is a delay (Δt) of 10 ± 2 ns between the time at which the input reaches pull-in level and the point at which the device output begins to rise (see Methods and Supporting Figure S7). Note that the rise time of the output voltage (i.e., the response following the initial delay of Δt) is limited by the buffer circuit used to characterize the device, not the device itself. (D) 'On' (black) and 'off' (gray) current for the device shown in (A) measured every 1,000 cycles (see Supporting Figure S4) for one million cycles. (E) Scanning electron micrograph of another cantilevered CNT NEM switch. Substrate is tilted 52° about the horizontal axis of the image. A Raman spectral map is overlaid where the intensity is the integrated area of the G-peak region. Spectra were obtained at 0.15 μm intervals using a 532 nm laser. Scale bar is 500 nm. (F) Raman spectrum from the marked point along the CNT in the map in (E). Black line is a Gauss-Lorentz fit to the D, G, D' and G' bands.

initiates in the input signal, the time resolution of the oscilloscope (10^9 samples/sec), and uncertainty in the buffer delay (see Supporting Information). Dynamic multiphysics models[18] predict a response time of approximately 6.6 ns for a device with geometry equivalent to the cantilevered device shown in Figure 2A, which serves as a complementary lower bound on the response time for this device (see Supporting Figure S8).

The long-term durability of the cantilevered devices was next characterized. The voltage was alternatingly stepped above the pull-in voltage and below the pull-out voltage. At intervals of 1,000 cycles, the 'on' and 'off' current was read at a voltage of V_{READ} = 22 V ($V_{PO} < V_{READ} < V_{PI}$, see Supporting Figure S4). Figure 2F shows the measured 'on' and 'off' current of the cantilevered switch shown in Figure 2A through 10^6 cycles. Consistent 'on' currents of 3.7 ± 0.3 nA were observed, with 'off' currents slightly above the noise floor.

Doubly-clamped (suspended) carbon-carbon NEM switches (**Figure 3**A) were also characterized. The response time was estimated using the same method as the cantilevered devices (see Supporting Figure S7) and found to be 12 ± 2 ns (Figure 3B). In general, the doubly-clamped boundary conditions of the suspended switches make for a stiffer structure[38] than a cantilevered switch of the same length, and should thus enable a faster response. However, the suspended switch tested (Figure 3A) was nearly 5 times longer in length than the cantilevered switch (Figure 2A), giving it a similar natural frequency.

Qualitatively, the current-voltage response of the suspended NEM switches was similar to that of the cantilevered switches as expected, and proved to be similarly repeatable. Figure 3C shows the full current-voltage response measured at select intervals of cycling (again cycling was done by alternatingly stepping the applied voltage above the pull-in voltage and below the pull-out voltage as for the cantilevered device). Through this period of cycling, V_{PI} decreased monotonically by approximately 0.5 V (~1%) over the first 10^3 cycles before remaining stable for the remainder of the 10^5 cycles (see Supplementary Figure S5). Similarly, V_{PO} decreased ~2% before stabilizing. This initial "break-in" period in which the pull-in and pull-out voltages decrease slightly is consistent with other reported work[18] and is believed to be the result of gradual removal of contaminants on the surface of the CNT and electrode. These contaminants, which could be residues from the fabrication process or deposited during SEM imaging, could slightly stiffen the CNT resulting in an elevated V_{PI}, or increase adhesion between the CNT and DLC electrode, resulting in an elevated V_{PO}. With repeated cycling, these contaminants likely wear or burn away, leaving behind the more stable pristine CNT and DLC surfaces.

While the short-term durability of these devices has been attributed to the low CNT-DLC adhesion and high electrical contact resistance which reduces the potential for harmful electrical discharge,[18] the long-term high-cycle reliability is

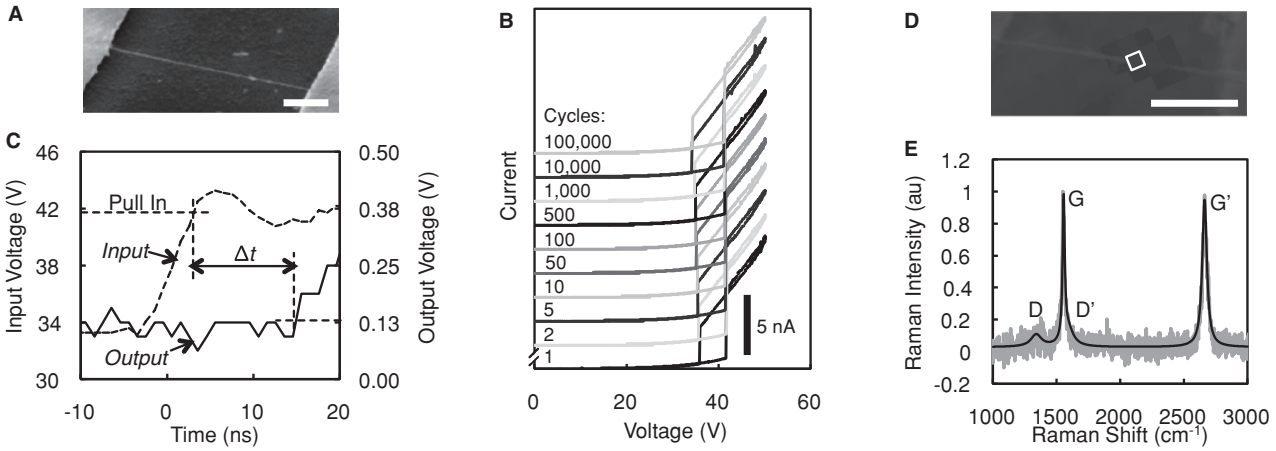

Figure 3. Characterization of suspended carbon-carbon NEM switches. (A) Scanning electron micrograph showing a suspended device. The CNT is fixed at both ends by palladium contacts and suspended over a DLC electrode. Scale bar is 500 nm. Sample is tilted 52° about the horizontal axis of the image. (B) Current-voltage response of the device shown in (A) with repeated cycling. Curves are staggered along the vertical axis for clarity (on an absolute scale, all start from the same point (0, 0)). (C) Plot of step input signal and switch output from the device shown in (A). Response time (Δt) is determined as in Figure 2C to be 12 ± 2 ns. Note that the rise time of the output voltage (i.e., the response following the initial delay of Δt) is limited by the buffer circuit used to characterize the device, not the device itself. (D) Scanning electron micrograph of another suspended CNT switch. Substrate is titled 45° about the horizontal axis of the image. A Raman spectral map is overlaid where the intensity is the integrated area of the G-peak region. Spectra were obtained at 0.15 µm intervals using a 532 nm laser. Scale bar is 1 µm. (E) Characteristic Raman spectrum from the marked point along the CNT in the map in (D). Black line is a Gauss-Lorentz fit to the D, G, D', and G' bands (see Supporting Figure S3).

hypothesized to be due to a combination of factors in the CNT-DLC carbon-carbon contact. On the electrode side of the contact, the extremely hard and smooth surface of the DLC is expected to reduce the propensity for wear-based degradation such as that observed with softer electrode coatings.[5] RMS surface roughness was measured to be 5 Å (Supporting Figure S9). An indentation hardness and Young's modulus on the order of 50 and 500 GPa, respectively, have also been reported for DLC.[39] As a result, these materials are widely pursued as robust coatings for their outstanding tribological properties (wear coefficient approximately 20 times lower than materials such as titanium nitride[39]). Other hard, electrically conductive materials, such as silicon carbide,[2] have similarly proven very durable for NEM device applications. In addition, while the large electrical contact resistance reduces short-term catastrophic failure due to electrical discharge and associated Joule heating,[18] it also reduces the possibility of more gradual pitting of the electrode surface or damage to the CNT.

On the CNT side of the contact, flexure of a pristine CNT during switch actuation should result primarily in distributed elastic strain of the C-C bonds (as is the case in RF applications where CNT resonators[40] routinely endure numerous cycles of similar strains in short periods without failure as they resonate in the absence of physical contact with an opposing electrode). Confocal Raman spectroscopy was used to assess the quality of the CNTs used (see Supporting Information). In general, CNTs produced by the arc discharge method, such as those used in this study, are considered to be of high quality with low defect density.[41,42] Figure 2E,F and Figure 3D,E show characteristic results in which the Raman spectra were mapped along individual cantilevered and suspended CNTs respectively. The low D-band intensity (a disorder- or defect-induced feature) and strong symmetry on the in-plane tangential G-band (i.e., minimal contribution from the D'-band which appears as a shoulder on the G-band and is a double resonance feature induced by disorder or defects) suggest a nearly pristine graphitic lattice structure in the CNTs.[43] This further suggests that the fabrication process used to construct the devices does not damage the CNTs.

As an example of the functionality of the carbon-carbon NEM switches, diode-resistor-type logic gates[44] were constructed from a pair of cantilevered NEM switches (**Figure 4**, and see further details in Supporting Information). The two CNTs were tied together electrically while the DLC electrodes associated with each switch were independently addressable and taken as the inputs (Figure S6). The electrical potential of the pair of CNTs (V_O), computed based upon the measured current through the resistor (see Supporting Information), is taken as the output. For example, AND gates were constructed by applying a fixed bias to the CNTs through a pull-down resistor and using the potential of the two electrodes as the inputs (Figure 4H). OR gates were constructed by grounding the CNTs through a pull-up resistor and again using the electrode potentials as the inputs (Figure 4I). The on-off ratio of the OR gate was approximately 1500. The AND gate exhibited a lower on-off ratio of 1.5, as it is largely limited by the high CNT-electrode contact resistance which prevents the CNT potential from being pulled fully down to ground when making contact with a grounded DLC electrode. As such, the reliable switching afforded by the carbon-carbon contact allows for demonstrations of functionality such as these logic gates. Future advances to various multi-electrode device architectures[17,45] will enable complete, ultra-compact logic families using far fewer elements than common CMOS-based logic. These switches however will likely see more widespread application in hybrid NEM-CMOS devices as a means to reduce the rapidly growing power

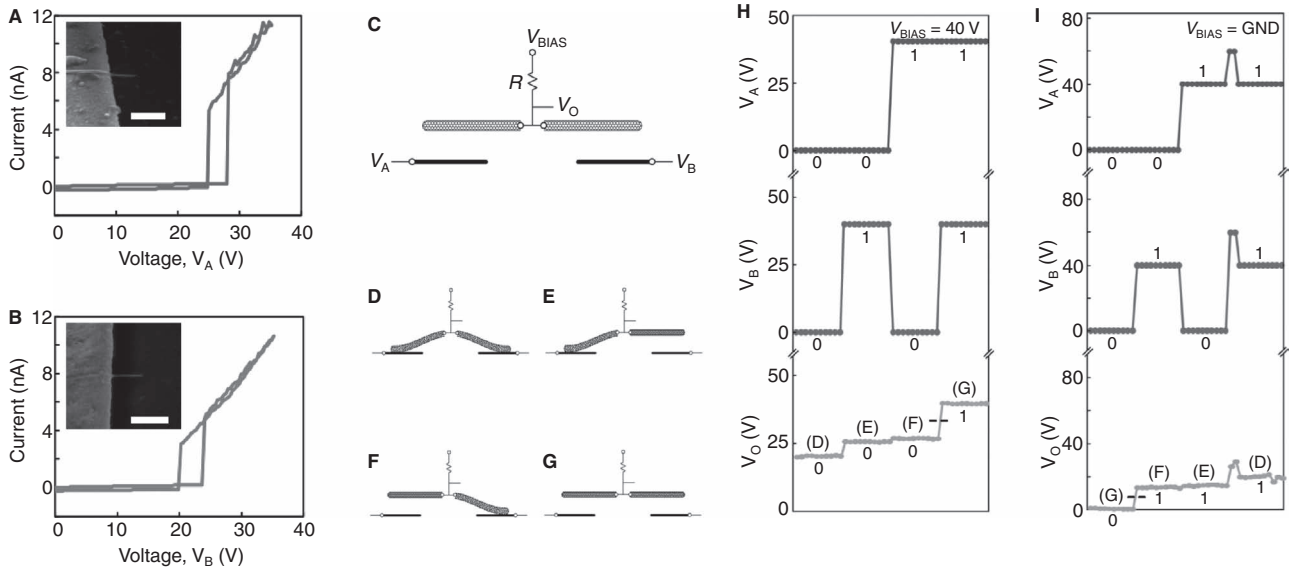

Figure 4. Logic gates constructed from pairs of carbon-carbon NEM switches. (A,B) Individual current-voltage responses of the two cantilevered NEM switches paired together to construct logic gates. Insets show scanning electron micrographs of the devices used. Scale bars are 500 nm. Substrate is tilted 52° with respect to the horizontal axis of the images. (C) Schematic of the pair of cantilevered devices as they are used for logic operations. The inputs to the two CNTs are tied together and biased through a resistor, while their DLC electrodes are independently addressable. The electrical potential of the CNTs, V_O, is taken as the output. (D-G) Schematics of the various states of the two NEM switches corresponding to the input combinations as labeled in (H,I). (H) Voltage inputs (V_A and V_B) and output (V_O) for an AND gate. (I) Inputs and output for an OR gate.

consumption of CMOS technologies will allowing for continued scaling of the silicon processes.[3,7,8]

In summary, the improved reliability demonstrated herein (thanks to a facile change in material selection), when combined with previously demonstrated ultra-low off currents and future advances in manufacturing to facilitate faster speeds and lower pull-in voltages, provides a path toward realizing highly sought after hybrid NEM-CMOS devices. These hybrid devices will consume significantly less power than their conventional CMOS counterparts, while allowing for continued scaling of the silicon.

The devices reported herein had response times around 10 ns and actuation voltages of 20 to 40 V, which are high relative to current CMOS. However, dynamic multi-physics models[18] predict that the response time can be reduced to approximately 1.5 ns for a device with the same geometry of that in Figure 2A but with only three CNT shells (see Supporting Figure S8). More significant reductions of one order of magnitude or more in both response time and pull-in voltage are expected by scaling down the critical dimensions (CNT length and diameter, and CNT-electrode gap) and by replacing the multi-walled CNTs used herein with single- or double-walled CNTs.[25,26] Dadgour et al. predict a target design window for cantilevered CNT NEM switches with lengths of 22 nm (equivalent to the most recent CMOS node technologies) and CNT-electrode gaps between 1 and 2 nm.[25] These devices would have pull-in voltages of around 1 V and speeds in the GHz range.

By combining NEM architectures with CMOS, hybrid technologies will combine the ultra-low leakage of NEM switches with the high 'on' currents of CMOS transistors.[3] While the off currents here were on the order of 10–100 pA (limited by the experimental fabrication and characterization methods used), on/off current ratios as high as 10^7 have been reported for NEM switches,[27] making them attractive candidates to reduce leakage in these hybrid systems. In addition, future optimization of the CNT-DLC contact in these devices will reduce the contact resistance (the primary limiter of 'on' current) to increase throughput and speed while maintaining device robustness. The current carrying capacity of the NEM switches themselves can also be greatly increased by employing arrays of switches in parallel, or through devices in which ensembles of many CNTs deflect together in the active element.[46]

Experimental Section

See detailed description of experimental materials and methods in the Supporting Information.

Supporting Information

Supporting Information is available from the Wiley Online Library or from the author.

Acknowledgements

HDE gratefully acknowledges support from the National Science Foundation through award Nos. CMMI-0555734 and DMR-0907196, the Army Research Office through award No. W911NF-08-1-0061, and the Office of Naval Research through award No. N00014-08-1-0792. This work was performed in part at the Center for Nanoscale Materials (CNM) which is supported by the U. S. Department of Energy, Office of Basic Energy Sciences under Contract No. DE-AC02–06CH11357, and in part at the Center for Integrated Nanotechnologies (CINT), a

U. S. Department of Energy, Office of Basic Energy Sciences user facility at Los Alamos National laboratory (Contract DE-AC52–06NA25396) and Sandia National Laboratories (Contract DE-AC04 — 94AL85000). The authors are grateful to Yehea Ismail and Joseph Friedman for their constructive review of the manuscript. OL gratefully acknowledges the Northwestern University Presidential and Ryan Fellowships.

Received: December 21, 2012
Revised: February 20, 2012
Published online: April 10, 2012

[1] T. Rueckes, K. Kim, E. Joslevich, G. Y. Tseng, C. Cheung, C. M. Lieber, *Science* **2000**, *289*, 94.
[2] T.-H. Lee, S. Bhunia, M. Mehregany, *Science* **2010**, *329*, 1316.
[3] H. F. Dadgour, K. Banerjee, *Comp. Digital Techniques, IET* **2009**, *3*, 593.
[4] J. Jang, S. Cha, Y. Choi, G. Amaratunga, D. Kang, D. Hasko, J. Jung, J. Kim, *Appl. Phys. Lett.* **2005**, *87*, 163114.
[5] W. Jang, J. Lee, J.-B. Yoon, M.-S. Kim, J.-M. Lee, S.-M. Kim, K.-H. Cho, D.-W. Kim, D. Park, W.-S. Lee, *Appl. Phys. Letts.* **2008**, *92*, 103110.
[6] S. Chong, K. Akarvardar, R. Parsa, J.-B. Yoon, R. T. Howe, S. Mitra, H.-S. P. Wong, in *Proceedings of the 2009 International Conference on Computer-Aided Design* **2009**, San Jose, California: ACM.
[7] H. F. Dadgour, K. Banerjee, in *44th ACM/IEEE Design Automation Conference* **2007**.
[8] Y. Zhou, S. Thekkel, S. Bhunia, in *Proceedings of the 2007 international symposium on Low power electronics and design* **2007**, Portland, OR, USA: ACM.
[9] M. N. Lovellette, A. B. Campbell, H. L. Hughes, R. K. Lawerence, J. W. Ward, M. Meinhold, T. R. Bengtson, G. F. Carleton, B. M. Segal, T. Rueckes, in *Aerospace Conference, 2004. Proceedings. 2004 IEEE* **2004**.
[10] L. Jonsson, S. Axelsson, T. Nord, S. Viefers, J. Kinaret, *Nanotechnology* **2004**, *15*, 1497.
[11] W. W. Jang, J.-B. Yoon, M.-S. Kim, J.-M. Lee, S.-M. Kim, E.-J. Yoon, K. H. Cho, S.-Y. Lee, I.-H. Choi, D.-W. Kim, D. Park, *Solid-State Electron.* **2008**, *52*, 1578.
[12] J. Kinaret, T. Nord, S. Viefers, *Appl. Phys. Lett.* **2003**, *82*, 1287.
[13] R. Smith, T. Rueckes, S. Konsek, J. Ward, D. Brock, B. Segal, in *IEEE Aerospace Conference* **2007**, Big Sky, MT.
[14] W. Xiang, C. Lee, *Appl. Phys. Lett.* **2010**, *96*, 193113.
[15] Q. Li, S.-M. Koo, M. Edelstein, J. Suehle, C. Richter, *Nanotechnology* **2007**, *18*, 315202.
[16] K. Ziegler, D. Lyons, J. Holmes, D. Erts, B. Polyakov, H. Olin, K. Svensson, E. Olsson, *Appl. Phys.Lett.* **2004**, *84*, 4074.
[17] H. F. Dadgour, M. M. Hussain, C. Smith, K. Banerjee, in *47th ACM/IEEE Design Automation Conference* **2010**.
[18] O. Loh, X. Wei, C. Ke, J. Sullivan, H. Espinosa, *Small* **2011**, *7*, 79.
[19] J.-W. Han, J.-H. Ahn, M.-W. Kim, J. Lee, J.-B. Yoon, Y.-K. Choi, *Small* **2010**, *6*, 1197.
[20] J. Jang, S. Cha, Y. Choi, D. Kang, T. Butler, D. Hasko, J. Jung, J. Kim, G. Amaratunga, *Nat. Nanotechnol.* **2008**, *3*, 26.
[21] S. Lee, D. Lee, R. Morjan, S. Jhang, M. Sveningsson, O. Nerushev, Y. Park, E. Campbell, *Nano Lett.* **2004**, *4*, 2027.
[22] H. F. Dadgour, M. M. Hussain, K. Banerjee, in *16th ACM/IEEE international symposium on Low power electronics and design* **2010**, Austin, Texas.
[23] C. Chen, R. Parsa, N. Patil, S. Chong, K. Akarvardar, J. Provine, D. Lewis, J. Watt, R. Hower, H. S. P. Wong, S. Mitra, in *18th annual ACM/SIGDA international symposium on Field programmable gate arrays* **2010**, Monterey, California, USA.
[24] International Roadmap Committee, *The international technology roadmap for semiconductors* **2009**.
[25] H. Dadgour, A. M. Cassell, K. Banerjee, in *IEEE International Electron Devices Meeting* **2008**.
[26] M. Yousif, P. Lundgren, F. Ghavanini, P. Enoksson, S. Bengtsson, *Nanotechnology* **2008**, *19*, 285204.
[27] Y. Hayamizu, T. Yamada, K. Mizuno, R. Davis, D. Futaba, M. Yumura, K. Hata, *Nat. Nanotechnol.* **2008**, *3*, 289.
[28] S. Axelsson, E. Campbell, L. Jonsson, J. Kinaret, S. Lee, Y. Park, M. Sveningsson, *New J. Phys.* **2005**, *7*, 1.
[29] C. H. Ke, H. D. Espinosa, *Small* **2006**, *2*, 1484.
[30] A. Subramanian, L. Dong, B. Nelson, A. Ferreira, *Appl. Phys. Lett.* **2010**, *96*, 073116.
[31] S. Cha, J. Jang, Y. Choi, G. Amaratunga, D. J. Kang, D. Hasko, J. Jung, J. Kim, *Appl. Phys.Lett.* **2005**, *86*, 083105.
[32] E. Dujardin, V. Derycke, M. Goffman, R. Lefevre, J. Bourgoin, *Appl. Phys.Lett.* **2005**, *87*, 193107.
[33] M. Siegal, T. Friedmann, J. Sullivan, J. Mikkalson, F. Dominquez, S. Kurtz, D. Tallant, R. Simpson, K. McCarty, L. Bernardex, D. Dibble, P. Mirkarimi, *Diamond and diamond-like carbon films for advanced electronic applications* **1996**.
[34] Z. Chen, J. J. Zhao, T. Yano, T. Ooie, M. Yoneda, J. Sakakibara, *J. Appl. Phys.* **2000**, *88*, 2305.
[35] C. H. Ke, H. D. Espinosa, N. Pugno, *J. Appl. Mech.* **2005**, *72*, 726.
[36] C. H. Ke, N. Pugno, B. Peng, H. D. Espinosa, *J. Mech. Phys. Solids* **2005**, *53*, 1314.
[37] A. Kaul, E. Wong, L. Epp, B. Hunt, *Nano Lett.* **2006**, *6*, 942.
[38] N. Pugno, C. H. Ke, H. D. Espinosa, *J. Appl. Mech.* **2005**, *72*, 445.
[39] F. Präßler, W. Grimm, T. Chudoba, *Plasma Processes Polym.* **2009**, *6*, S468.
[40] V. Sazonova, Y. Yaish, H. Ustunel, D. Roundy, T. Arias, P. McEuen, *Nature* **2004**, *431*, 284.
[41] N. Grobert, *Mater. Today* **2007**, *10*, 28.
[42] A. Felten, C. Bittencourt, J.-J. Pireaux, M. Reichelt, J. Mayer, D. Hernandez-Cruz, A. P. Hitchcock, *Nano Lett.* **2007**, *7*, 2435.
[43] V. Datsyuk, M. Kalyva, K. Papagelis, J. Parthenios, D. Tasis, A. Siokou, I. Kallitsis, C. Galiotis, *Carbon* **2008**, *46*, 833.
[44] P. Horowitz, W. Hill, *The Art of Electronics,* Cambridge University Press, **1980**.
[45] S.-J. Choi, J.-H. Ahn, J.-W. Han, M.-L. Seol, D.-I. Moon, S. Kim, Y.-K. Choi, *Nano Lett.* **2011**, *11*, 854.
[46] J. W. Ward, M. Meinhold, B. M. Segal, J. Berg, R. Sen, R. Sivarajan, D. K. Brock, T. Rueckes, in *Non-Volatile Memory Technology Symposium* **2004**.
[47] F. Wakaya, K. Katayama, K. Gamo, *Microelectron. Eng.* **2003**, 67–68, 853.
[48] C. Lan, P. Amama, T. Fisher, R. Reifenberger, *Appl. Phys. Lett.* **2007**, *91*, 093105.
[49] S. Dohn, K. Mølhave, P. Bøggild, *Sens. Lett.* **2005**, *3*, 300.
[50] B. Peng, M. Locascio, P. Zapol, S. Li, S. L. Mielke, G. C. Schatz, H. D. Espinosa, *Nat. Nanotechnol.* **2008**, *3*, 626.